Model Predictive Control of Grid-tied Photovoltaic Systems: Maximum Power Point Tracking and Decoupled Power Control

Mohammad B. Shadmand[1], *Student Member, IEEE*, Xiao Li[2], *Student Member, IEEE*, Robert S. Balog[3], *Senior Member, IEEE*, and Haitham Abu Rub[4], *Senior Member, IEEE*
Renewable Energy & Advanced Power Electronics Research Laboratory[1-3]
Dept of Electrical & Computer Engineering, Texas A&M University, College Station, USA[1-3]
Dept of Electrical & Computer Engineering, Texas A&M University at Qatar, Doha, Qatar[4]
mohamadshadmand@gmail.com[1], xiaoli1.tamu@gmail.com[2], robert.balog@ieee.org[3], haitham.abu-rub@qatar.tamu.edu[4]

***Abstract* — This paper presents maximum power point tracking (MPPT) and decoupled power control for single phase grid-tied photovoltaic (PV) systems. Model predictive control (MPC) technique is used to extract the maximum power from the PV array and feed it to grid. The stochastic behavior of solar energy necessitates MPPT of PV system to operate at maximum power point and make the system economical. Power control of grid-tied inverters are commonly based on synchronous reference frame transformation, this methodology requires the phase angle information by phase-looked loop (PLL). In this paper MPC technique is used for decoupled active and reactive power control of the single phase grid-tied inverter. The proposed technique does not need PLL, modulation module and synchronization transform, which makes the control algorithm simple for digital implementation. Comparing the developed technique to the conventional perturb & observe (P&O) method indicates significant improvement in PV system performance. The simulation result is validated by implementing the control algorithm experimentally using dSPACE 1007.**

I. Introduction

The reduction in the cost of photovoltaic (PV) cells has increased interest in this renewable energy source with installed PV capacity growing at an annual rate of 60% from 2004 to 2009, and 80% recently [1]. However the low conversion efficiency of PV cells remain a significant obstacle to their wide spread use [2]. Due to the high variability of the solar energy resource [3, 4], maximum power point tracking (MPPT) is required to ensure continuous operation at the maximum power point [5-9] and harvest maximum energy.

Several MPPT techniques have been investigated over the past couple of decades; the relative merits of these various methods are explored in [6]. The critical operating regime is low solar irradiance level. Harvesting all of the available solar energy during low solar irradiance periods can substantially improve system performance. An effective MPPT controller and converter can use available energy to significantly reduce the amount of installed PV.

Considering the MPPT methods discussed in [6], candidate techniques considered include Incremental Conductance (INC) [5], Perturb-and-Observe (P&O) [10], fractional Open-Circuit Voltage (Voc) [11], and Best Fixed Voltage (BFV) [3]. Each approach has certain advantages and disadvantages. P&O is a well-known technique with relatively good performance; however, P&O method cannot always converge to the true maximum power point. Also, P&O is relatively slow, which limits its ability to track transient solar irradiance conditions. One of the contributions of this paper is to improve the P&O method performance by predicting the error one step ahead in horizon through model predictive control technique for grid connected PV system. The proposed method has faster response than conventional P&O under rapidly changing atmospheric conditions.

The PV array can feed power to the grid through a DC/DC converter boosting the output voltage and a grid connected inverter. A flyback converter is chosen as a DC/DC converter in this paper. The output power of the flyback converter is fed to ac grid through an inverter controlled by predictive model based decoupled power control.

Many power control strategies for the single-phase inverter have been proposed over the past few decades [12-15]. In general, the control process requires the amplitude and phase angle information of the AC mains voltage captured by the phase-looked loop (PLL). However, the PLL module, as a nonlinear part, usually degrades the output performance of system [16]. In addition, some other modules are necessary for this application such as: properly tuned synchronous reference frame (SRF) based PI controller, pulse width modulation (PWM), and dc-link capacitor voltage control. Designs of these modules are challengeable to get the desired performance. Consequently, it will be good if a new control method is proposed to implement without these modules, which can make the control algorithm simpler and reduce cost of the design.

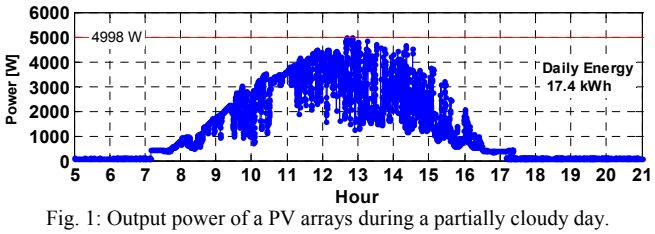

Fig. 1: Output power of a PV arrays during a partially cloudy day.

978-1-4673-6765-3/15/$31.00 ©2015 IEEE

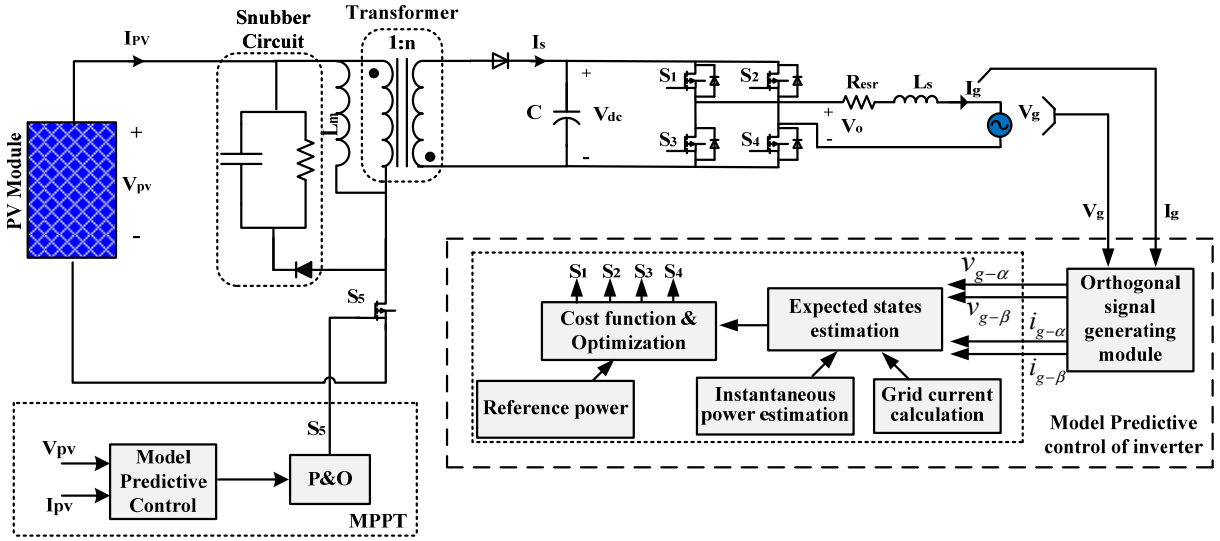

Fig. 2: General schematic of the system and proposed model predictive control for grid connected PV system.

The proposed method based on MPC is straightforward and completely eliminates the need for PI controllers and a modulation stage. In this paper, the MPC concept is extended for decoupled real and reactive power control of single-phase grid-tied inverter. In the proposed controller, active power and reactive power of inverter are considered to be controlled independently and flexibly. In the proposed controller, the synchronization function is embedded into the power control process; therefore, the PLL unit is not required. Modulation module is not needed in the proposed approach by MPC which reduce the complexity of designing the system. The results show that the proposed controller has good steady-state and dynamic performance. Fig. 2 illustrates the general schematic of the complete grid connected PV system controlled by predictive methods.

II. Principle of Model Predictive Control

Application of model predictive control (MPC) in power electronics with low switching frequency dates back to the 1980's for high power applications [17, 18]. Since high switching frequencies for the MPC algorithm required long calculation time, widespread adoption was not feasible at that time. In the past decade, with the improvement of high speed microprocessors, interest in the application of MPC in power electronics with high switching frequency has increased considerably [7, 8, 19].

The main characteristic of MPC is predicting the future behavior of the desired control variables [18, 19] until a specific time in the horizon. The predicted control variables are used to obtain the optimal switching state by minimizing a cost function. The discrete time model of the control variables used for prediction can be presented as a state space model as follows [18]:

$$x(k+1) = Ax(k) + Bu(k) \quad (1)$$

$$y(k) = Cx(k) + Du(k) \quad (2)$$

A cost function that takes into consideration the future states, references, and future actuations can then be defined [18]:

$$g = f(x(k), u(k), \cdots, u(k+N)) \quad (3)$$

The defined cost function g should be minimized for a predefined length in the time horizon N; a sequence of N optimal actuations will be determined where the controller only applies the first element of sequence:

$$u(k) = \begin{bmatrix} 1 & 0 & \cdots & 0 \end{bmatrix} \arg\min_{u} g \quad (4)$$

At each sampling time the optimization problem is solved again by using a new set of measured data to obtain a new sequence of optimal actuation.

The general scheme of MPC for power electronics converters is illustrated in Fig. 3 [19]. In this block diagram measured variables, $X(K)$, are used in the model to estimate predictions, $\tilde{X}(K+1)$, of the controlled variables for all of the n possible switching states. These predictions are then evaluated using a cost function which compares them to the reference values, $X^*(K+1)$, by considering the design constraints. Finally the optimal actuation, S, is selected and applied to the converter. The general form of the cost function, g, subject to minimization can be formulated as

$$g = \left[\tilde{X}_1(K+1) - X_1^*(K+1)\right] + \lambda_1\left[\tilde{X}_2(K+1) - X_2^*(K+1)\right] + \ldots + \lambda_n\left[\tilde{X}_n(K+1) - X_n^*(K+1)\right] \quad (5)$$

where λ is the value or weight factor for each objective.

III. Maximum Power Point Tracking Using Model Predictive Control

A flyback converter is chosen as a DC/DC converter. P&O determines the reference current for the MPC which determines the next switching state, Fig. 4 [20]. This technique predicts the error of the next sampling time and based on optimization of the cost function g, illustrated in Fig. 5, the

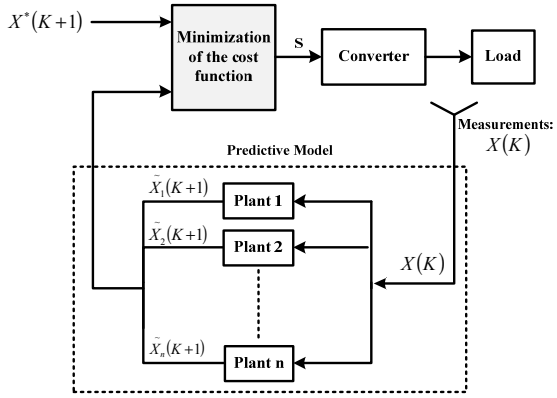

Fig. 3. MPC general schematic for power electronics converters.

switching state will be determined. The inputs to the predictive controller are the PV system current, voltage, and the reference current. By deriving the discrete time set of equations, the behavior of control variable can be predicted at next sampling time *k*. The proposed methodology is based on the fact that the slope of the PV array power curve is zero at the predicted MPP, positive on the left and negative on the right of the predicted MPP.

The discrete time set of equations of the flyback converter shown in Fig. 2 is given by (2) and (3) when switch is "ON" and (4) and (5) when switch is "OFF" [21]:

$$i_{PV}(k+1) = \frac{T_S}{L} v_{PV}(k) + i_{PV}(k) \tag{6}$$

$$v_C(k+1) = \left(1 - \frac{T_S}{RC}\right) v_C(k) \tag{7}$$

$$i_{PV}(k+1) = i_{PV}(k) - \frac{T_S}{Ln} v_C(k) \tag{8}$$

$$v_C(k+1) = \frac{T_S}{nC} i_{PV}(k) + \left(1 - \frac{T_S}{RC}\right) v_C(k) \tag{9}$$

Now after determination of the reference current using the procedure shown in Fig. 4, the cost function can be obtained as following

$$g_{S=0,1} = \left| i_{PV_{S=0,1}}(k+1) - i_{ref} \right| \tag{10}$$

The objective is to minimize the cost function *g*. The final switching state for MPPT can be determined using procedure illustrated in Fig. 5.

IV. Model Predictive Decoupled Power Control

The conventional H-bridge grid tied inverter configuration is illustrated in Fig. 2. There are numerous examples in the literature of inverter topologies capable of feed power produced from renewable sources to the ac power grid [14, 22-25]. Table 1 provides a list of the output voltage V_o as a function of switching states and the function $\psi(t)$ which provides the desired polarity of the output voltage. The state of the switches are represented by 0 and 1, where state 0 means the switch is OFF, and state 1 means the switch is ON. The discrete-time model of inverter is derived as:

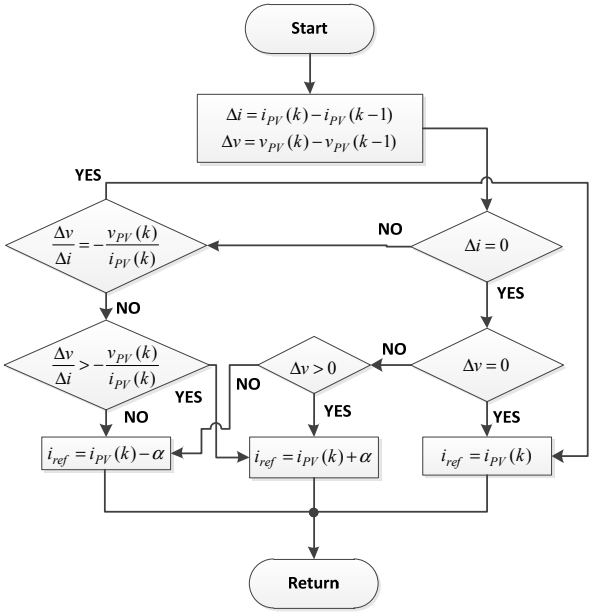

Fig. 4. MPC procedure to determine reference current using P&O

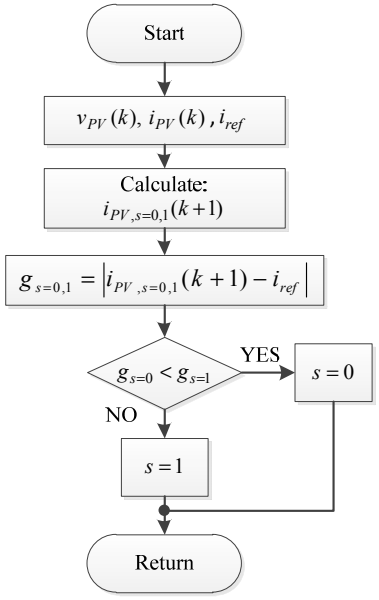

Fig. 5. MPC-MPPT procedure

Table 1: switching states of the grid-tied inverter.

	S_1	S_2	S_3	S_4	Ψ	V_o
State 1	0	0	1	1	0	0
State 2	1	1	0	0	0	0
State 3	1	0	0	1	1	V_{dc}
State 4	0	1	1	0	-1	$-V_{dc}$

$$i_g(k+1) = \frac{T_s}{L}(V_0(k) - V_g(k) - i_g(k) \times R_{esr}) + i_g(k) \tag{11}$$

$$V_o = \psi(t) \times V_{dc} \tag{12}$$

where: $\psi(t) = S_1(t)S_4(t) - S_2(t)S_3(t)$

In order to control the output reactive power value of single-phase grid-connected inverter, an extra module orthogonal signal generation (OSG) is needed to create orthogonal signal of the grid voltage current. With this process,

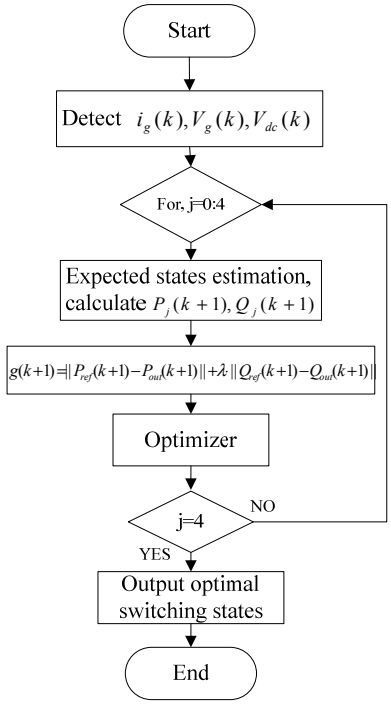

Fig. 6. MPC procedure for decoupled power control.

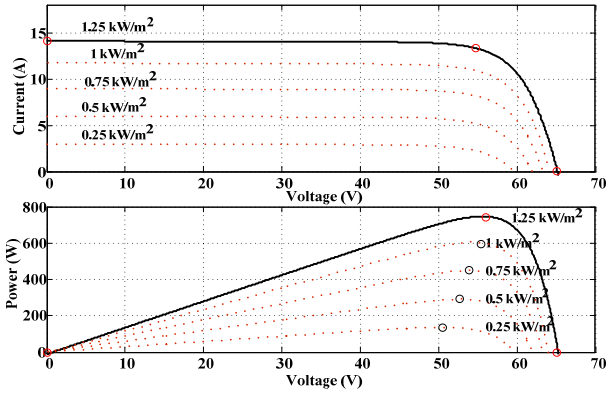

Fig. 7. I-V and P-V characteristics of the array.

the grid reactive power values can be calculated based on instantaneous power theory as

$$P=\frac{1}{2}(V_{g-\alpha}\times I_{g-\alpha}+V_{g-\beta}\times I_{g-\beta}) \quad (13)$$

$$Q=\frac{1}{2}(V_{g-\beta}\times I_{g-\alpha}-V_{g-\alpha}\times I_{g-\beta}) \quad (14)$$

where $V_{g\text{-}\alpha}$ and $V_{g\text{-}\beta}$ are the output signals of the OSG module with V_g input, and $I_{g\text{-}\alpha}$ and $I_{g\text{-}\beta}$ are the output signals of the OSG module with I_g input.

The cost function g subject to minimization which include active and reactive power can be formed as

$$g(k+1)=|P_{ref}(k+1)-P_{out}(k+1)|+\lambda\cdot|Q_{ref}(k+1)-Q_{out}(k+1)| \quad (15)$$

The detail algorithm of the control is illustrated in Fig. 6. The reference reactive power is provided by the grid operator. The determined maximum power point by MPPT from the PV array is the command for active power.

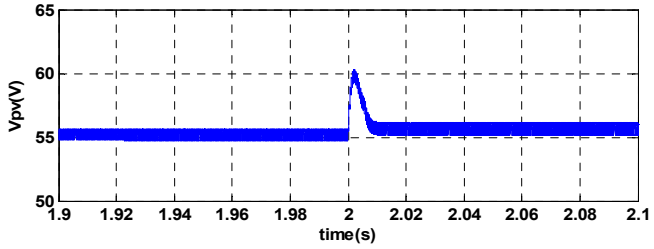

Fig. 8. PV side voltage by proposed MPC-MPPT

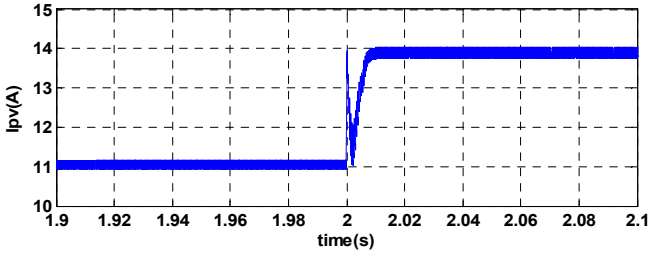

Fig. 9. PV side current by proposed MPC-MPPT.

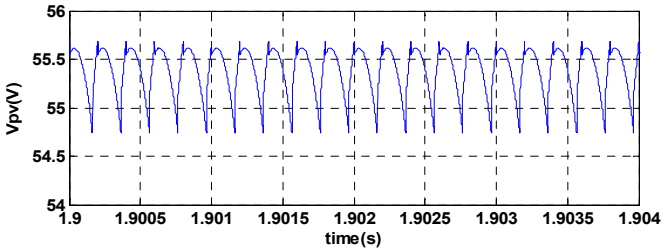

Fig. 10. PV voltage ripple at 1000 W/m^2 irradiance.

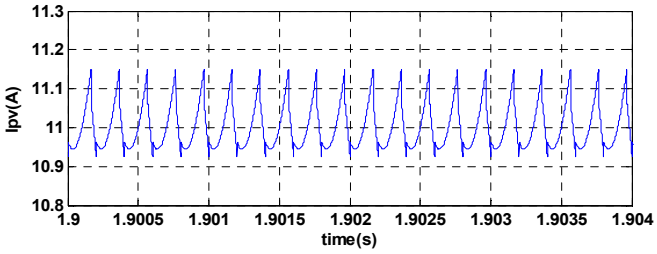

Fig. 11. PV current ripple at 1000 W/m^2 irradiance.

V. Results and Discussion

The proposed controller for the PV system is modeled in MATLAB-Simulink, and implemented in dSPACE ds1007. The I-V and P-V characteristic of the PV systems used in this paper for different irradiance levels are illustrated in Fig. 7. The SUNPOWER SPR-305-WHT is used as PV module type. The sampling time, T_s, is 10 µs. In this paper the model predictive control for MPPT is compared to the commonly used P&O method. Figs. 8-11 illustrate the simulation results of the proposed MPC-MPPT. The system is tested under two irradiance level changes, at time 2 s, the irradiance level changed from 1000 W/m^2 to 1250 W/m^2. The proposed MPC-MPPT has faster dynamic performance when comparing to the conventional P&O method as illustrated in Figs. 12 and 13. By considering continuous operation of the PV systems over the year, the extra amount of energy captured by the proposed MPPT technique is significant, particularly under the cloudy sky condition.

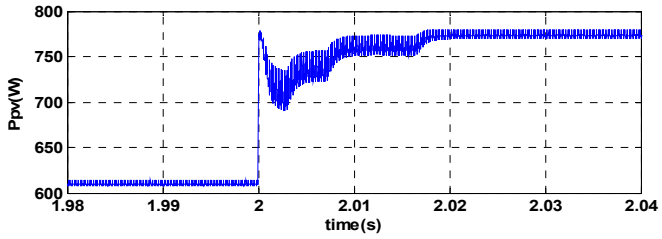

Fig. 12. PV side power by proposed P&O-MPPT

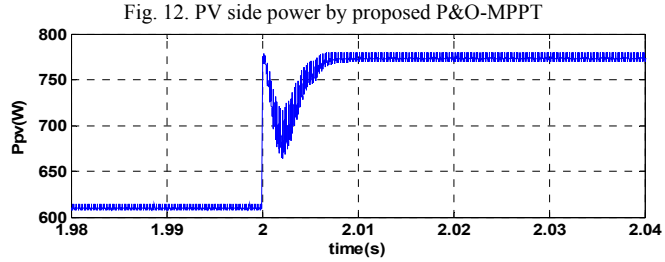

Fig. 13. PV side power by proposed MPC-MPPT

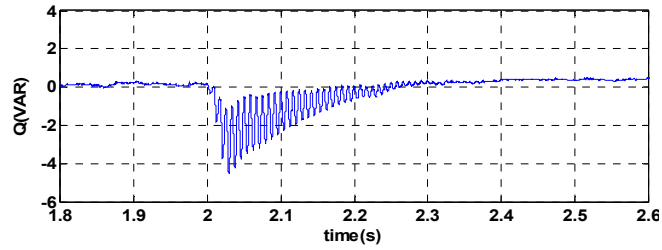

Fig. 14. Output reactive power (grid side).

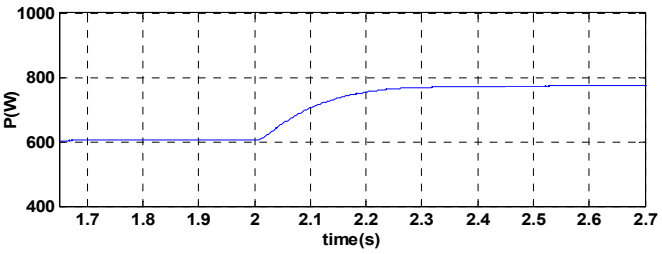

Fig. 15. Output real power (grid side).

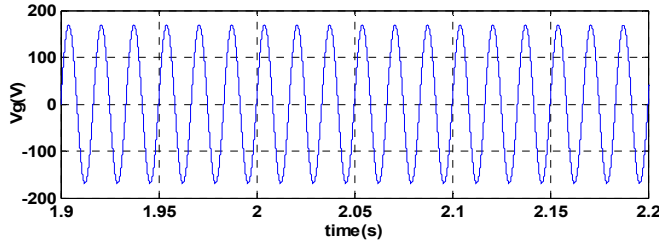

Fig. 16. Grid side voltage.

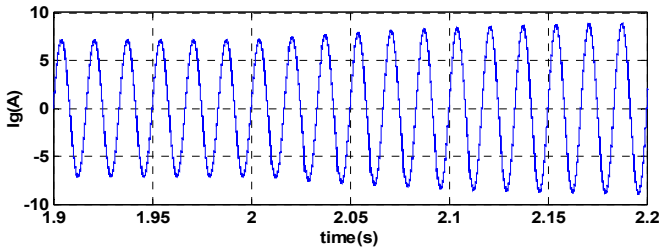

Fig. 17. Grid side current.

The simulation results of the grid side voltage, current, and power using MPC decoupled power control are illustrated in

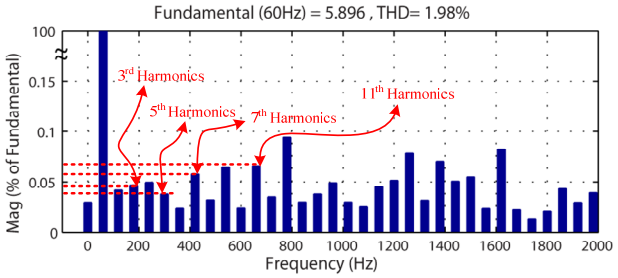

Fig. 18. Spectrum analysis of grid side current.

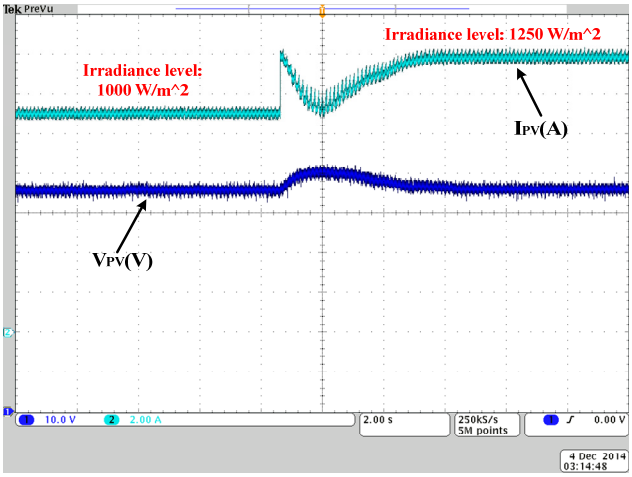

Fig. 19. PV side voltage and current by MPC-MPPT.

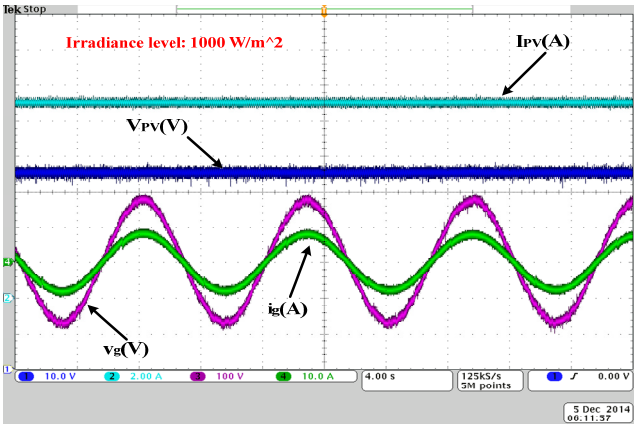

Fig. 20. Grid and PV side voltage and current at 1000 W/m^2 irradiance.

Figs. 14-17, for step change in solar irradiance level from 1000 W/m^2 to 1250 W/m^2. The reference reactive power is zero and the reference active power determined based on the MPP at PV side, as illustrated, unity power factor is achieved. The THD of the grid side current is about 1.98% which is within the IEEE-519 standard [26], Fig. 18. The simulation results are validated experimentally by real-time implementation of the control strategy with dSPACE ds1007, Figs. 19 and 20. The experimental FFT analysis illustrated in Fig. 21 to validate the simulation results.

VI. Conclusion

This paper presents a MPPT technique that uses MPC to predict the error at the next sampling time, before applying the

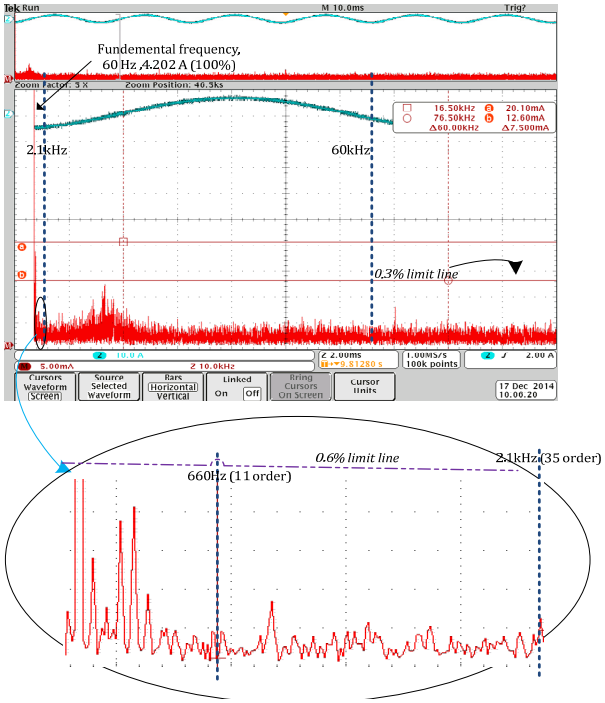

Fig. 21. FFT analysis of grid side current.

switching signal. MPC is also used for ac output power control of a single-phase grid-tied inverter and is implemented without needing a PLL for synchronization. The proposed predictive MPPT technique is compared to the P&O method and shows the benefits and improvements in the speed and efficiency of the MPPT. The results show that for the same steady state error, the MPP is tracked much faster by using the MPC technique than P&O method. The dSpace ds1007 is used for experimental demonstration the control techniques.

ACKNOWLEDGMENT

This publication was made possible by NPRP grant # 4-077-2-028 from the Qatar National Research Fund (a member of Qatar Foundation). The statements made herein are solely the responsibility of the authors.

VII. REFRENCES

[1] Z. Peng, W. Yang, X. Weidong, and L. Wenyuan, "Reliability Evaluation of Grid-Connected Photovoltaic Power Systems," *IEEE Transactions on Sustainable Energy,* vol. 3, pp. 379-389, 2012.

[2] M. Kasper, D. Bortis, T. Friedli, and J. W. Kolar, "Classification and comparative evaluation of PV panel integrated DC-DC converter concepts," in *IEEE Pow. Elec. and Motion Cont. Conf. (EPE/PEMC)*, 2012.

[3] D. Sera, T. Kerekes, R. Teodorescu, and F. Blaabjerg, "Improved MPPT Algorithms for Rapidly Changing Environmental Conditions," in *IEEE Pow. Elec. and Motion Cont. Conf. (EPE-PEMC)*, 2006, pp. 1614-1619.

[4] M. B. Shadmand, R. S. Balog, and M. D. Johnson, "Predicting Variability of High-Penetration Photovoltaic Systems in a Community Microgrid by Analyzing High-Temporal Rate Data," *IEEE Transactions on Sustainable Energy,* vol. 5, pp. 1434-1442, 2014.

[5] A. Bidram, A. Davoudi, and R. S. Balog, "Control and Circuit Techniques to Mitigate Partial Shading Effects in Photovoltaic Arrays," *IEEE Journal of Photovoltaics,* vol. 2, pp. 532-546, 2012.

[6] T. Esram and P. L. Chapman, "Comparison of Photovoltaic Array Maximum Power Point Tracking Techniques," *IEEE Transactions on Energy Conversion,* vol. 22, pp. 439-449, 2007.

[7] M. Shadmand, R. S. Balog, and H. Abu Rub, "Maximum Power Point Tracking using Model Predictive Control of a flyback converter for photovoltaic applications," in *IEEE Power and Energy Conference at Illinois (PECI)*, 2014, pp. 1-5.

[8] M. B. Shadmand, M. Mosa, R. S. Balog, and H. A. Rub, "An Improved MPPT Technique of High Gain DC-DC Converter by Model Predictive Control for Photovoltaic Applications," in *IEEE Applied Power Electronics Conference & Exposition (APEC)*, 2014, pp. 2993 - 2999.

[9] A. R. Kashyap, R. Ahmadi, and J. W. Kimball, "Input voltage control of SEPIC for maximum power point tracking," in *IEEE Power and Energy Conference at Illinois (PECI)*, 2013, pp. 30-35.

[10] N. Femia, G. Petrone, G. Spagnuolo, and M. Vitelli, "Optimization of perturb and observe maximum power point tracking method," *IEEE Transactions on Power Electronics,* vol. 20, pp. 963-973, 2005.

[11] K. A. Kim, R. M. Li, and P. T. Krein, "Voltage-offset resistive control for DC-DC converters in photovoltaic applications," in *IEEE Applied Power Electronics Conference and Expo. (APEC)*, 2012, pp. 2045-2052.

[12] R. Bojoi, L. R. Limongi, D. Roiu, and A. Tenconi, "Enhanced Power Quality Control Strategy for Single-Phase Inverters in Distributed Generation Systems," *IEEE Transactions on Power Electronics,* vol. 26, pp. 798-806, 2011.

[13] M. Aleenejad, H. Iman-Eini, and S. Farhangi, "Modified space vector modulation for fault-tolerant operation of multilevel cascaded H-bridge inverters," *IET Power Electronics,* vol. 6, pp. 742-751, 2013.

[14] M. Aleenejad, R. Ahmadi, and P. Moamaei, "A modified selective harmonic elimination method for fault-tolerant operation of multilevel cascaded H-bridge inverters," in *Power and Energy Conference at Illinois (PECI)*, 2014, pp. 1-5.

[15] M. Hamzeh, S. Farhangi, and B. Farhangi, "A new control method in PV grid connected inverters for anti-islanding protection by impedance monitoring," in *IEEE Workshop on Control and Modeling for Power Electronics (COMPEL)*, 2008, pp. 1-5.

[16] Z. Qi, S. Xiang-Dong, Z. Yan-Ru, M. Matsui, and R. Bi-Ying, "Analysis and Design of a Digital Phase-Locked Loop for Single-Phase Grid-Connected Power Conversion Systems," *IEEE Transactions on Industrial Electronics,* vol. 58, pp. 3581-3592, 2011.

[17] J. Holtz and S. Stadtfeld, "A predictive controller for the stator current vector of AC machines fed from a switched voltage source," in *International Power Electronics Conf. (IPEC)*, 1983, pp. 1665–1675.

[18] J. Rodriguez and P. Cortes, *Predictive control of power converters and electrical drives* vol. 37: John Wiley & Sons, 2012.

[19] J. Rodriguez, M. P. Kazmierkowski, J. R. Espinoza, P. Zanchetta, H. Abu-Rub, H. A. Young, *et al.*, "State of the Art of Finite Control Set Model Predictive Control in Power Electronics," *IEEE Transactions on Industrial Informatics,* vol. 9, pp. 1003-1016, 2013.

[20] M. B. Shadmand, R. S. Balog, and H. Abu-Rub, "Model Predictive Control of PV Sources in a Smart DC Distribution System: Maximum Power Point Tracking and Droop Control," *IEEE Transactions on Energy Conversion,* vol. 29, pp. 913-921, 2014.

[21] R. W. Erickson and D. Maksimovic, *Fundamentals of power electronics*: Kluwer Academic Pub, 2001.

[22] S. Sajadian and E. C. dos Santos, "Three-phase DC-AC converter with five-level four-switch characteristic," in *Power and Energy Conference at Illinois (PECI)*, 2014, pp. 1-6.

[23] E. C. dos Santos Junior and S. Sajadian, "Energy conversion unit with optimized waveform generation," in *IEEE Industry Applications Society Annual Meeting*, 2013, pp. 1-6.

[24] B. Farhangi and S. Farhangi, "Application of Z-source converter in photovoltaic grid-connected transformer-less inverter," *Electrical Power Quality and Utilisation, Journal,* vol. 12, 2006.

[25] S. Harb, M. Kedia, Z. Haiyu, and R. S. Balog, "Microinverter and string inverter grid-connected photovoltaic system-A comprehensive study," in *IEEE Photovoltaic Specialists Conference (PVSC)*, 2013, pp. 2885-2890.

[26] C. K. Duffey and R. P. Stratford, "Update of harmonic standard IEEE-519: IEEE recommended practices and requirements for harmonic control in electric power systems," *IEEE Transactions on Industry Applications,* vol. 25, pp. 1025-1034, 1989.